The Astrophysical Journal, 792:36 (10pp), 2014 September 1 doi:10.1088/0004-637X/792/1/36

COMPARISON OF TWO-FLUID AND GYROKINETIC MODELS FOR KINETIC ALFVÉN WAVES IN SOLAR AND SPACE PLASMAS

L. Yang[1,2], D. J. Wu[1], S. J. Wang[2], and L. C. Lee[3]
[1] Purple Mountain Observatory, Chinese Academy of Sciences, Nanjing 210008, China; ylei@pmo.ac.cn
[2] Key Laboratory of Solar Activity, National Astronomical Observatories, Chinese Academy of Sciences, Beijing 100012, China
[3] Institute of Earth Sciences, Academia Sinica, Taipei, Taiwan
Received 2014 February 19; accepted 2014 July 16; published 2014 August 12

ABSTRACT

An analytical comparative study of a two-fluid and a gyrokinetic model of kinetic Alfvén waves (KAWs) is presented for various solar and space plasma environments. Based on the linear KAW dispersion relation for gyrokinetics (Howes et al. 2006), the wave group velocity and electromagnetic polarizations are obtained analytically. Then the gyrokinetic wave properties are compared with those of the two-fluid model. The results show that both models agree well with each other not only in the long wavelength regime ($\gg$ the ion gyroradius ρ_i) for all cases considered, but also in wavelengths $\sim\rho_i$ and $\ll\rho_i$ (still much larger than the electron gyroscale) for a moderate or low ($\lesssim 1$) and a high ($\gg 1$) ion/electron temperature ratio T_{0i}/T_{0e}, respectively. However, the fluid model calculations deviate strongly from the gyrokinetic model at scales $< \rho_i$ for a relatively low T_{0i}/T_{0e} due to the electron gyroradius effect. Meanwhile, the plasma β_i can make the gyrokinetic dispersion relation of KAWs become complex and sometimes have an oscillation-like structure. With the inherent simplicity of the fluid theory, these results may improve our understanding of the applicability of the two-fluid model, and may have important implications for computer simulation studies of KAWs in the solar and space plasma surroundings.

Key words: methods: analytical – plasmas – waves

1. INTRODUCTION

When the ion Larmor radius (or ion gyroscale, ρ_i) effect is considered, Alfvén waves are no longer decoupled from the rest of the plasma dynamics, and have changes in density and magnetic field strength. Such Alfvén waves are called kinetic Alfvén waves (KAWs; Hasegawa & Uberoi 1982) or dispersive Alfvén waves (Stasiewicz et al. 2000), and are of major importance for particle acceleration and heating in solar and space plasmas due to the strongly anisotropic characteristics of the wave electromagnetic polarizations and spatially magnetized structures (see, for example, a recent book by Wu 2013 and references therein). It has been shown that the polarization of KAWs depends sensitively on the local plasma parameters such as the ion/electron temperature ratio, the plasma kinetic/magnetic pressure ratio β ($= 2\mu_0 n(T_i + T_e)/B^2$), and their transverse wavenumber $k_\perp\rho_i$ (e.g., Hasegawa & Chen 1975; Hasegawa & Uberoi 1982; Lysak & Lotko 1996; Howes et al. 2006; Schekochihin et al. 2009; Hollweg 1999; Wu 2003; Chen & Wu 2011). KAWs were introduced into space plasma physics by Hasegawa (1976) to consider the effects of finite electron pressure and finite ion gyroradius on the ideal MHD shear Alfvén waves. The electron pressure and ion gyroradius can increase the parallel phase velocity of the wave, while the electron inertia decreases the parallel phase velocity (e.g., Lysak & Lotko 1996). Both of the inertial and kinetic limits of the Alfvén wave dispersion relation have been discussed in detail (e.g., Hasegawa & Uberoi 1982; Goertz 1984). For typical parameters along auroral field lines, the inertial limit was appropriate below about 4–5 R_E, while the kinetic limit was more appropriate above that altitude (Lysak & Carlson 1981). In these aurora regions, observations of KAWs have been obtained from sounding rockets (Boehm et al. 1990) and the *Freja* satellite (Wahlund et al. 1994; Louarn et al. 1994; Boehm et al. 1995). KAWs have also been well identified in ionosphere (Chaston et al. 2006), near and within the plasma sheet-tail lobe boundary (Wygant et al. 2000). These waves could be excited by mode conversion from surface waves on the plasma sheet boundary (Hasegawa 1976), the refraction of Alfvén waves (e.g., Heyvaerts & Priest 1983; Ofman & Davila 1995), or the resonant absorption (Ionson 1978) under different plasma conditions.

One of the most important features of KAWs is that the wave electric field fluctuations parallel to the background magnetic field $\mathbf{B}_0$ are capable of leading to Landau damping and plasma heating (Stéfant 1970; Dobrowolny & Torricelli-Ciamponi 1985; Lysak & Lotko 1996; Leamon et al. 1999; Hollweg 1999), so such waves are of interest in various situations involving strong gradients transverse to $\mathbf{B}_0$, parallel electric fields, and plasma energization (Hui & Seyler 1992; Hasegawa & Mima 1978). Related examples of applications are the Earth's aurora (e.g., Hasegawa 1976; Goertz 1984, 1985; Kletzing 1994; Wang et al. 1996; Thompson & Lysak 1996; Wu & Chao 2003) and substorms (Goertz & Smith 1989), planetary magnetospheres (Farrell et al. 1992; Das & Ip 1992), comets (Sharma & Papadopoulos 1995), extragalactic jets (Bodo & Ferrari 1982; Jafelice & Opher 1987), solar radio bursts (Treumann et al. 1990; de Assis & Leubner 1994), solar flares (Kuts & Iukhimuk 1990; de Assis & de Azevedo 1993), minor heavy ion acceleration in coronal holes (Yang & Wu 2005; Wu & Yang 2006, 2007) and the heating of solar coronal loops (Ionson 1978; Wentzel 1979; Assis & Busnardo-Neto 1987; Voitenko et al. 1990; Iukhimuk & Kuts 1990; de Assis & Tsui 1991; Kucherenko & Yukhimuk 1993; de Azevedo et al. 1994).

Recently, many studies show that KAWs are closely related with turbulence and are believed to be important to support turbulent energy cascade in the solar wind and in other astrophysical plasmas (i.e., Schekochihin et al. 2009; Podesta et al. 2010; Chandran et al. 2011; Kumar Dwivedi & Sharma 2013 and references therein), and to be responsible for the density

fluctuation spectra observed at large wavenumbers and the cascade of kinetic turbulence in the corona and in the solar wind (Hollweg 1999; Chandran et al. 2009; Howes et al. 2012). Whether a KAW cascade can reach electron scales in the solar wind was discussed by Podesta et al. (2010) and Howes et al. (2011b). Based on linear solutions of the Vlasov kinetic theory, Sahraoui et al. (2012) considered the relevance of various plasma modes in carrying the energy cascade down to electron scales and concluded that the KAW branch is the more relevant candidate to carry the energy cascade down to electron scales than the whistler branch in this cascade energy transfer process, which is also supported by the observations of the solar wind turbulence (Howes et al. 2011b; Salem et al. 2012; Howes et al. 2012). In short, theoretical and empirical evidence also suggests that the major part of the energy in solar wind turbulence is in the form of low-frequency anisotropic KAW fluctuations that are not subject to ion cyclotron damping (Howes & Quataert 2010). However, an observational study on the role of KAWs and cyclotron damping in the solar wind does not support the exclusive KAW interpretation generally applied to high-β solar wind intervals but does support the presence of cyclotron damping at a significant level (Smith et al. 2012). The damping mechanisms of the solar wind turbulence are generally complex and require more efforts to be resolved with great clarity.

The main physical properties of KAWs (i.e., the dispersion relation, propagation, and electromagnetic polarizations) can be described by the two-fluid and kinetic or gyrokinetic equations to be introduced in the following. The two-fluid description assumes that the velocity distribution function of the particles (protons and electrons) is isotropic and the particles can be described by the equations for ideal fluids in a self-consistent way. The fluid models can provide a reasonably approximate description of the plasma behavior, the development of which has a rich history in plasma and space physics. By treating protons and electrons separately, the two-fluid description allows for the finite inertial effects of the individual particle species. Several early publications (e.g., Schlüter 1950; Spitzer 1956; Bernstein & Trehan 1960) have discussed the approximations made in the basic two-fluid equations. The two-fluid dispersion relation for fast, slow, and Alfvén waves with frequencies below the electron plasma frequency was given by Braginskii (1957), Stringer (1963), and Formisano & Kennel (1969). Also, the two-fluid equations were used by Stringer (1963) to investigate the propagation of low-frequency plane waves in a low-β, homogeneous, collisionless plasma with a scalar pressure, constant temperature, infinite electrical conductivity, and zero viscosity. In an infinite, uniform, high-β plasma, Formisano & Kennel (1969) utilized the same two-fluid model to obtain the phase velocities and polarizations of linear waves and found that the features of high-β plasma waves differ from those of low-β ones. Although the two-fluid approach cannot yield the Landau damping due to resonant particles (i.e., Sagdeev & Shafranov 1958; Lysak & Lotko 1996; Hollweg 1999), the general dispersion and wave properties derived from the two-fluid approach are in good agreement with those of the more exact, but much less tractable, kinetic theory. Such fluid models can still be useful to understand which wave type and wavenumber is best suited to extract energy from the particle velocity distribution under investigation by giving correctly the velocity and general properties of the various possible waves (Stringer 1963).

Various two-fluid models have been examined to further include more complex effects and to interpret some relevant observations in astrophysical plasmas. From two-fluid equations, Cao & Kan (1987) shown that the finite Larmor radius effect is responsible for the field-aligned currents in the fast and slow modes and for the compressibility in the Alfvén mode, which may explain the time-dependent field-aligned current sheets related with ion gyroscale auroral arcs. Base on a finite-temperature two-fluid plasma model with an adiabatic equation of state, Lyu & Kan (1989) obtained a comprehensive set of nonlinear one-dimensional constant-profile isentropic hydromagnetic wave solutions to demonstrate the high-degree of alignment of the wave normal with the local average magnetic field in the solar wind. Passot & Sulem (2006) constructed the fluid model keeping hydrodynamic nonlinearities and a linear approximation of the Landau damping and of the finite Larmor radius effect to study the mirror mode dynamics. Besides, the two-fluid theory was also used to investigate the magnetorotational instability—one of the most important processes in astrophysics, with applications ranging from accretion disks to entire galaxies (Ferraro 2007; Ren et al. 2011), to illustrate the long-lived corotating high speed solar wind streams and short-lived phenomena (Metzler et al. 1979), and to support the important role played by Alfvén wave turbulence in the solar wind (Chandran et al. 2011).

To reduce the complexities in the kinetic description, the fluid description of KAWs has also been developed widely due to its simplicity and intuition. A magnetohydrodynamic model of KAWs with finite ion gyroradius through the ion stress tensor was used by Marchenko et al. (1996) to interpret ultra low frequency wave phenomena in the Earth's magnetosphere. A two-fluid model was also employed by Hollweg (1999) to study the KAWs' compressibility and electromagnetic polarizations, which show that the wave becomes strongly compressive when the perpendicular wavelength is of the order of the ion inertial length, accompanied by a parallel magnetic field fluctuation such that the total pressure perturbation $\approx$0. From the exact two-fluid model, Wu (2003) derived a general dispersion equation to show that both the ion temperature and inertia can affect well the behavior of the KAW's propagation, resonance, and polarization. In addition, two-fluid simulations for the generation of KAWs by a rotating magnetic field source showed good agreement with experimental measurements (Karavaev et al. 2011).

On the other hand, the kinetic description of KAWs (i.e., Hasegawa & Chen 1975; Hasegawa 1976; Lysak & Lotko 1996) can provide important kinetic effects such as Landau damping and gyroradius orbit averaging. In particular, Lysak & Lotko (1996) considered the KAW dispersion relation including full kinetic effects for both electrons and ions, and found that the Landau damping is not important for the perpendicular wavelength larger than the ion acoustic gyroradius and the electron inertial length, and that ion gyroradius effects can reduce the Landau damping by raising the parallel phase velocity of the wave above the electron thermal speed in the short perpendicular wavelength regime. For obliquely propagating KAWs in a wide range of interplanetary conditions, numerical solutions of the linearized Maxwell–Vlasov equations demonstrated that electron Landau damping plays a significant role for the heating of thermal electrons in interplanetary magnetic field fluctuations (Leamon et al. 1999).

As a low-frequency limit of the kinetic theory based on averaging over the gyration of charged particles about a mean magnetic field (i.e., a description of charged rings moving in the ring-averaged electromagnetic fields), gyrokinetic theory has been developed intensively in the past (e.g., Rutherford &

Frieman 1968; Taylor & Hastie 1968; Catto 1978; Frieman & Chen 1982; Dubin et al. 1983; Brizard 1992). The gyrokinetic approach orders out fast MHD waves and the cyclotron resonance, but retains finite Larmor radius effect and collisionless wave–particle interactions via the Landau resonance (Landau 1946; Barnes 1966). It was recognized to be appropriate for the study of astrophysical plasmas, including galaxy clusters, accretion disks around compact objects, the interstellar medium, solar corona, and solar wind (Howes et al. 2006, 2008a; Schekochihin et al. 2009). In this regard, a concise review and a detailed derivation of gyrokinetics were provided by Howes et al. (2006), and a general theoretical framework of gyrokinetics (Schekochihin et al. 2009) and a gyrokinetic simulation code, AstroGK (Numata et al. 2010), have been developed to understand plasma turbulence in astrophysical plasmas. Using this code, gyrokinetic numerical simulations were employed to test the ability of a weakened cascade model to predict the properties of the turbulent steady-state in a weakly collisional plasma (Numata et al. 2010), and to explain the nearly power-law energy spectra observed in the dissipation range of both kinetic numerical simulations and solar wind observations (Howes et al. 2011a). Besides, gyrokinetic simulations are also used to study collisionless reconnection with a large guide field regime in relevant solar corona and solar wind environment (TenBarge et al. 2014) and the linear tearing instability (Numata et al. 2011), where highly detailed and reliable results were provided.

As far as KAWs are concerned, AstroGK was performed to describe the transition from Alfvén to KAW turbulence at the scale of the ion Larmor radius to understand the solar wind turbulence (Howes et al. 2008b), and to study the KAW properties in the Large Plasma Device experiment (Nielson et al. 2010). Three-dimensional nonlinear gyrokinetic simulations of plasma turbulence resolving scales from the ion to electron gyroradius showed that the linear KAW mode can quantitatively describe the polarization of the nonlinear turbulent fluctuations (Howes et al. 2011b), and quantitatively reproduce the magnetic energy exponential spectrum in the solar wind, indicating that a turbulent cascade of KAWs is sufficient to explain the observed magnetic energy spectrum in the dissipation range of solar wind turbulence (TenBarge et al. 2013).

The main reason for the present comparative study is that for practical or computational purposes, a fluid model is simpler and faster to evolve numerically, although in principle, a kinetic approach would seem closer to the real world and can provide a rigorous treatment of the physics for the complex aspects of particle–field interactions (Song et al. 2008; Lee & Büchner 2010; Diomede et al. 2008; Echim et al. 2011). Fluid models may be thought to be inferior to kinetic ones, but this is not the case in general. Obtaining actual numerical solutions to a kinetic model is more difficult and computationally slower for a realistic plasma system (Alexashov & Izmodenov 2005; Song et al. 2008; Diomede et al. 2008; Echim et al. 2011), and equations of a kinetic description can only be solved numerically or analytically in very simple situations (such as steady state, one-dimensional, collisionless flows). Given the complexity and technical difficulties in solving kinetic equations, an adequate fluid description could be used to eliminate some of this computational complexity (Song et al. 2008; Echim et al. 2011), and be applied to the detailed nonlocal or global analysis of plasma stability (Janaki et al. 2012; Lee & Büchner 2010) and more complicated geometries (including two-dimensional and three-dimensional cases; Lee & Büchner 2010; Echim et al. 2011) for interpretation of observational results.

The fluid and kinetic or gyrokinetic models have been compared in many previous publications. Krauss-Varban et al. (1994) compared the general mode properties of low-frequency waves in kinetic theory with those in two-fluid theory, and found that at small wavenumbers, the kinetic mode properties typically start to deviate significantly from their fluid counterparts at $\beta \sim 0.5$. At larger β, there is no longer a consistent correspondence between the fluid and kinetic modes. The validity of Hall MHD for turbulence in weakly collisional plasmas was shown by Howes (2009) from a quantitative comparison with Vlasov–Maxwell kinetic theory over a wide range of parameter space. Using the hot two-fluid and the Vlasov theories, Sahraoui et al. (2012) studied key properties of the linear plasma modes with highly oblique angles of propagation under realistic solar wind conditions at 1 AU. Recently, the complementarity of the fluid and kinetic approaches has been discussed by Parker (2010) to study the coronal expansion and solar wind. Two-fluid and kinetic models were also compared to show agreement with some limits for steady magnetic reconnection (Brackbill 2011) and for the dynamics of convection in the inner magnetosphere (Song et al. 2008). With regard to KAWs, it has been shown that the wave dispersion relation in Hall MHD (one-fluid theory) can be recovered exactly from kinetic theory in the limit of cold ions and adiabatic electrons (Ito et al. 2004). Schekochihin et al. (2009) have proven that the validity of the two-fluid description does not depend on the assumption of high collisionality and can extend to scales well below the mean free path, but above the ion gyroscale. More recently, Hunana et al. (2013) compared the isotropic two-fluid model with the kinetic model, the usual double-adiabatic proton and electron model, and two different Landau fluid models to study the polarization and compressibility of oblique KAWs, concluding that kinetic effects cannot be ignored even for the wavelength much longer than the proton gyroscale. As far as we know, further detailed comparison on the KAW's properties is not provided between the two-fluid and gyrokinetic descriptions. Since both two-fluid (Wu 2003) and gyrokinetic (Howes et al. 2006) formalisms have been used to describe KAW dynamics, separately and independently, but to what degree they coincide with each other is not fully understood. Therefore, to provide a detailed comparison of analytical results between the two-fluid (Wu 2003) and gyrokinetic (Howes et al. 2006) models of KAWs is of much importance for the theoretical and simulation studies of waves in the solar and space plasmas.

With the recognition that the gyrokinetic description is more detailed, closer to physical reality than the two-fluid model, the wave properties of the two models will be compared analytically in some detail in this paper. There are two main aims for this research: (1) to explore the similarities and differences in both models for values that can be determined from available observations (e.g., the number density, temperature of particles, and magnetic fields) in the solar and space plasma environments, and (2) to check the validity and limits of the two-fluid model for KAWs. The results might possibly lead to future improvements in the simplified two-fluid models to make them more appropriate for dealing with some aspects of the KAW modeling and simulations applied to various observed solar and space plasma phenomena.

The rest of this paper is structured as follows. Sections 2 and 3 describe the two-fluid and gyrokinetic models of KAWs, respectively. The results of comparison between the two models are presented in Section 4, and the validity and limits of both models in some solar and space plasmas are discussed in

Section 5. The main results and conclusions are summarized in Section 6.

2. TWO-FLUID MODEL

From an exact two-fluid model, Wu (2003) derived a general dispersion equation and discussed the effects of ion temperature and inertia on the behavior of KAWs' propagation, resonance, and polarization. Using this model for KAWs in a low β_i ($\ll 1$) plasma with a homogeneous ambient magnetic field $\mathbf{B}_0$ oriented in the z direction, we can obtain the wave dispersion relation,

$$\bar{\omega}^2 = \frac{T_{0i}/T_{0e} + (1 + T_{0i}/T_{0e})\alpha_i}{(T_{0i}/T_{0e})\left[1 + \alpha_i \Big/ \left(\frac{\beta_i}{2}\frac{m_i}{m_e}\right)\right]}, \quad (1)$$

from a more complete form of the dispersion relation given by Wu (2003, see Equation (36) in that paper), where $\bar{\omega} \equiv \omega/k_\parallel v_A$, $\alpha_i = k_\perp^2 \rho_i^2/2$, ω is the wave frequency, $k_\parallel/k_\perp$ the components of the wave vector parallel/perpendicular to the ambient magnetic field, $v_A = B_0/(\mu_0 n_i m_i)^{1/2}$ the Alfvén speed, T the temperature, β the ratio of plasma pressure to magnetic pressure, m the mass of particles, ρ_i the ion Larmor radius, and the subscripts i and e denote protons and electrons, respectively. The positive dispersion is dominated by the electron and ion temperatures, and the negative dispersion by the inertia of both particles. The term $\alpha_i/(\beta_i m_i/2m_e)$ (i.e., $k_\perp^2\lambda_e^2$) in the denominator denotes the electron inertial effect, where λ_e is the electron skin depth or the electron inertial length. It should be noted that the finite frequency modification has been neglected, that is, the low-frequency limit ($\ll$ ion gyrofrequency) is chosen here to be consistent with the assumption of the gyrokinetics by Howes et al. (2006; see Equation (1) in the paper).

Then from the two-fluid equations in the paper of Wu (2003), it is easy to get the parallel group velocity

$$v_{g\parallel} \equiv \partial\omega/\partial k_\parallel = \bar{\omega} v_A, \quad (2)$$

the perpendicular group velocity

$$v_{g\perp} \equiv \partial\omega/\partial k_\perp = \frac{\left[(1 + T_{0e}/T_{0i})\frac{\beta_i}{2}\frac{m_i}{m_e} - 1\right]\alpha_i \Big/ \left(\frac{\beta_i}{2}\frac{m_i}{m_e}\right)}{[1 + (1 + T_{0e}/T_{0i})\alpha_i]\left[1 + \alpha_i \Big/ \left(\frac{\beta_i}{2}\frac{m_i}{m_e}\right)\right]} \times \bar{\omega}\cot\theta v_A, \quad (3)$$

the polarizations of the wave fields

$$\frac{E_z}{E_x} = \frac{\left(1 + \alpha_i - \frac{T_{0e}}{T_{0i}}\frac{\beta_i}{2}\frac{m_i}{m_e}\right)\alpha_i \Big/ \left(\frac{\beta_i}{2}\frac{m_i}{m_e}\right)}{(1 + \alpha_i)\left[1 + \alpha_i \Big/ \left(\frac{\beta_i}{2}\frac{m_i}{m_e}\right)\right]} \cot\theta, \quad (4)$$

and

$$\frac{E_x}{B_y} = \frac{(1 + \alpha_i)\left[1 + \alpha_i \Big/ \left(\frac{\beta_i}{2}\frac{m_i}{m_e}\right)\right]}{1 + (1 + T_{0e}/T_{0i})\alpha_i}\bar{\omega} v_A, \quad (5)$$

where θ is the angle between the wave vector $\mathbf{k}$ and the background magnetic field $\mathbf{B}_0$. The electromagnetic polarization states of KAWs is of crucial importance in wave–particle interactions because the electric field can accelerate particles along its own direction, but the related magnetic field scatters particles in the transverse direction, which may help to clarify the physical mechanism of the particle energization processes.

Here it should be pointed out that the short-wavelength (<ion inertial length) and low-frequency ($\ll$ion gyrofrequency) Alfvén waves propagate only in directions quasi-perpendicular (i.e., $k_\perp^2 \gg k_\parallel^2$ or $\tan^2\theta \gg 1$) to the background magnetic field in a low β plasma (e.g., Wu 2003; Bellan 2012), which is consistent with the basic assumptions of the gyrokinetic theory for KAWs (Howes et al. 2006). The consistency lays the basis for our comparative study on the two models.

3. GYROKINETIC MODEL

Here we will examine the physical properties of same KAWs as discussed in Section 2, but from a gyrokinetic point of view based on the work by Howes et al. (2006). In this paper, we consider two limits of interest: $(m_e/m_i)(T_{0i}/T_{0e}) \ll \beta_i \ll 1$ and $\beta_i \sim m_e/m_i \ll 1 \ll T_{0i}/T_{0e}$. The analytical expressions for the wave dispersion relation, the group velocity, and the corresponding electromagnetic polarizations are presented in the following.

3.1. For the Limit $(m_e/m_i)(T_{0i}/T_{0e}) \ll \beta_i \ll 1$

For weak damping, the dispersion relation (see Equation (D20) in Howes et al. 2006) is

$$\bar{\omega}^2 = \frac{\alpha_i\,[1 - \Gamma_0(\alpha_i) + T_{0i}/T_{0e}]}{(T_{0i}/T_{0e})B\Gamma_0(\alpha_e)}, \quad (6)$$

where $\alpha_e = k_\perp^2\rho_e^2/2$, $\Gamma_0(\alpha_{i,e}) = I_0(\alpha_{i,e})e^{-\alpha_{i,e}}$ arises from ring averages in gyrokinetics, $B = 1 - \Gamma_0(\alpha_i) + (T_{0i}/T_{0e})[1 - \Gamma_0(\alpha_e)]$, ρ_e is the electron Larmor radius, and I_0 is the modified Bessel function of the first kind of order zero. It is clear that the dispersion relation of KAWs is dominated by the temperature ratio T_{0i}/T_{0e}, and we call Equation (6) temperature-dominated dispersion relation. Because the two-fluid model presented in this paper only describes the wave properties without damping and the imaginary part, arising from the plasma dispersion function in the gyrokinetic expressions of KAWs, can be ignored for the weak damping case, it is possible for us to directly compare the fluid solutions with the related real part of the gyrokinetic solutions. As long as the damping rate is small compared to the real part of the frequency, then the remaining calculated wave properties from the two-fluid model may closely, though not exactly, resemble those in the nearly collisionless situations encountered in solar and space environment.

Differentiating the dispersion relation (6) with respect to $k_\perp$, we can obtain the wave group velocity

$$\frac{v_{g\perp}}{v_A} = \cot\theta\bar{\omega}\left\{1 + \alpha_i\left[\frac{\Gamma_1(\alpha_i)}{1 - \Gamma_0(\alpha_i) + T_{0i}/T_{0e}} - \frac{\Gamma_1(\alpha_i) + (m_e/m_i)\Gamma_1(\alpha_e)}{B} + \frac{m_e T_{0e}}{m_i T_{0i}}\frac{\Gamma_1(\alpha_e)}{\Gamma_0(\alpha_e)}\right]\right\}, \quad (7)$$

where $\Gamma_1(\alpha_{i,e}) = [I_0(\alpha_{i,e}) - I_1(\alpha_{i,e})]e^{-\alpha_{i,e}}$ is also from ring averages in gyrokinetics, and I_1 is the modified Bessel function of the first kind of order 1.

Similarly, the parallel group velocity is

$$v_{g\parallel} \equiv \frac{\partial\omega}{\partial k_\parallel} = \bar{\omega} v_A. \quad (8)$$

From the vector potential $\mathbf{A}$ and scalar potential ϕ, we can easily determine the magnetic and electric fields

$$\mathbf{B} = \nabla \times \mathbf{A}, \quad \mathbf{E} = -\nabla\phi - \frac{\partial \mathbf{A}}{\partial t}. \quad (9)$$

Note that all quantities are expressed in SI units in this paper. The related algebraic linear system of field equations can be written in matrix form (see Equation (C15) in Howes et al. (2006)) as

$$\begin{pmatrix} A & A-B & C \\ A-B & A-B-\frac{\alpha_i}{\bar{\omega}^2} & C+E \\ C & C+E & D-\frac{2}{\beta_i} \end{pmatrix} \begin{bmatrix} \hat{\phi} \\ -\frac{\omega \hat{A}_\parallel}{k_\parallel} \\ \left(\frac{T_{0i}}{q_i}\right)\frac{\hat{B}_\parallel}{B_0} \end{bmatrix} = 0, \quad (10)$$

where the particle charge $q_i = e$ is for protons, the symbol $\hat{}$ denotes the corresponding amplitudes of ϕ, $\mathbf{A}$, and $\mathbf{B}$. The coefficients A, B, C, D, and E are defined in the paper by Howes et al. (2006), so we do not write them out here for brevity.

In the limit $\beta_i \ll 1$, one has A, B, C, D, and $E \sim O(1)$. Therefore, we can reduce Equation (10) and get the following relation

$$\hat{\phi} = \left(1 - \frac{B}{A}\right)\frac{\omega}{k_\parallel}\hat{A}_\parallel, \quad (11)$$

and the perturbed parallel magnetic field $\mathbf{B}_\parallel = 0$. Then we introduce Cartesian coordinates with the y axis in the direction of $\mathbf{B}$ and the z axis along the background magnetic field (i.e., the direction denoted by the subscript "$\parallel$") for direct comparison with the results of the two-fluid model presented in Section 2.

The Coulomb gauge $\nabla \cdot \mathbf{A} = 0$ yields $A_\perp/A_\parallel = -k_\parallel/k_\perp = -\cot\theta$. Due to $\mathbf{k} \perp \mathbf{B}$, $\mathbf{k} \perp \mathbf{A}$, $\mathbf{A} \perp \mathbf{B}$, and $\mathbf{B} \perp B_0\hat{\mathbf{z}}$ (in the limit $\beta_i \ll 1$), vectors $\mathbf{A}$, $\mathbf{k}$, and $\mathbf{E}$ are all in the x–z plane. Fourier transforming Equation (9) and using Equation (11) and the Coulomb gauge $\nabla \cdot \mathbf{A} = 0$ can result in the ratio of parallel to perpendicular electric fields

$$\frac{E_z}{E_\perp} = \frac{E_z}{E_x} = -\frac{B/A}{\cot\theta + (1 - B/A)\tan\theta}, \quad (12)$$

where $A \simeq 1 - \Gamma_0(\alpha_i) + T_{0i}/T_{0e}$ (i.e., Equation (D18) in the work of Howes et al. (2006) for a weak damping case), and the subscript "$\perp$" denotes the direction (i.e., the x or y axis) perpendicular to the background magnetic field (i.e., the z axis). Then, Faraday's law gives

$$\frac{E_\perp}{B_\perp v_A} = \frac{E_x}{B_y v_A} = \frac{\bar{\omega}}{1 - \tan\theta\, E_z/E_x}. \quad (13)$$

It should be mentioned that $\mathbf{E} = E_x\,\hat{\mathbf{x}} + E_z\,\hat{\mathbf{z}}$, and $\mathbf{B} = B_y\,\hat{\mathbf{y}}$.

Substituting Equation (12) into Equation (13), we can get

$$\frac{E_x}{B_y v_A} = \bar{\omega}[1 - (B/A)\sin^2\theta]. \quad (14)$$

Note here that Equations (12) and (14) are general in the limit $\beta_i \ll 1$ for the gyrokinetic description of KAWs, and so are still valid in the limit $\beta_i \sim m_e/m_i \ll 1 \ll T_{0i}/T_{0e}$ to be discussed in Section 3.2.

3.2. For the Limit $\beta_i \sim m_e/m_i \ll 1 \ll T_{0i}/T_{0e}$

When $\beta_i \sim m_e/m_i \ll 1 \ll T_{0i}/T_{0e}$, the dispersion relation of KAWs with weak damping is

$$\bar{\omega}^2 = \frac{\alpha_i \Gamma_0(\alpha_e)(m_i/m_e)\beta_i}{[2\alpha_i + \Gamma_0(\alpha_e)(m_i/m_e)\beta_i]\,B}, \quad (15)$$

which is Equation (D24) in Howes et al. (2006), and B is the same as that in Equation (6) for the limit $(m_e/m_i)(T_{0i}/T_{0e}) \ll \beta_i \ll 1$. In this case the dispersion relation of KAWs is dominated by the inertial term m_i/m_e, because the temperature ratio T_{0i}/T_{0e} in B is not important for the dispersion at ion gyroscale. Therefore, we call Equation (15) the inertia-dominated dispersion relation.

Using Equation (15) and taking the same procedure as that used in Section 3.1, we can get the parallel group velocity $v_{g\parallel} = \omega/k_\parallel$ and the perpendicular group velocity

$$\frac{v_{g\perp}}{v_A} = \bar{\omega}\cot\theta\left\{1 - \left[\frac{\Gamma_1(\alpha_e)m_e T_{0e}}{\Gamma_0(\alpha_e)m_i T_{0i}} + \frac{2 - \Gamma_1(\alpha_e)(T_{0e}/T_{0i})\beta_i}{2\alpha_i + \Gamma_0(\alpha_e)(m_i/m_e)\beta_i} + \frac{\Gamma_1(\alpha_i) + (m_e/m_i)\Gamma_1(\alpha_e)}{B}\right]\alpha_i\right\}. \quad (16)$$

The polarization relations between the KAW electric and magnetic fields have the same forms as those in Section 3.1, that is, Equations (12) and (14). However, here

$$A \simeq B - \frac{\Gamma_0(\alpha_e)}{2\bar{\omega}^2}\frac{m_i}{m_e}\beta_i \quad (17)$$

(see Equation (D22) in the work of Howes et al. 2006) for KAWs with weak damping, i.e., the imaginary part has been omitted in all expressions due to its value much smaller than that of the corresponding real part.

4. RESULTS

To make a detailed comparison between the two-fluid and gyrokinetic models of KAWs, we perform some numerical calculations based on the analytical expressions in Sections 2 and 3. For a finite β_i limit (i.e., $(m_e/m_i)(T_{0i}/T_{0e}) \ll \beta_i \ll 1$, Figure 1), both models are qualitatively compatible with each other well for the normalized wave frequency $\omega/(k_\parallel v_A)$, wave group velocity $v_{g\perp}/v_A$, and electromagnetic polarizations $E_z/E_\perp$ and $E_x/(B_y v_A)$ for long wavelengths with $k_\perp\rho_i < 1$. However, the absolute value of the relative frequency difference $d\omega$ ($\equiv \omega_{2-\mathrm{fluid}}/\omega_{\mathrm{gyrokinetic}} - 1$) between the two-fluid and gyrokinetic models is about 10% at $k_\perp\rho_i = 1.68$, and becomes more obvious for short wavelengths with $k_\perp\rho_i > 1$. The negative $d\omega$ in the short wavelength regime indicates that the wave frequency derived from the two-fluid model is smaller than that from the gyrokinetic model. However, the gyrokinetic dispersion in this case overestimates the real frequency for low T_{0i}/T_{0e} (e.g., $T_{0i}/T_{0e} = 0.01$ or $\rho_i/\rho_e = 4.3$; see Figure 10 in Howes et al. 2006), so the actual difference between the two-fluid and the full gyrokinetic dispersion relations might be smaller than that presented here. Similar changes with the long and short wavelength ranges are found for the differences in $v_{g\perp}/v_A$, $E_z/E_\perp$, and $E_x/(B_y v_A)$ between the two models.

In the finite β_i limit, we further analytically compare the dispersion behavior of KAWs for both models in the short wavelength regime. For the low $T_{0i}/T_{0e} \ll 1$ limit, the two-fluid dispersion relation (1) becomes

$$\bar{\omega}^2_{2-\mathrm{fluid}} = \frac{\alpha_i}{(T_{0i}/T_{0e})\left[1 + \alpha_i/\left(\frac{\beta_i}{2}\frac{m_i}{m_e}\right)\right]}. \quad (18)$$

Further considering $k_\perp\rho_i \gtrsim 1$ (i.e., $\alpha_i \gtrsim 1$) and $k_\perp\rho_e \ll 1$ (i.e., $\alpha_e \ll 1$, and hence $\Gamma_0(\alpha_e \ll 1) \sim 1$) in the same temperature limit, from the gyrokinetic dispersion relation (6) we can obtain

$$\bar{\omega}^2_{\mathrm{gyrokinetic}} = \frac{\alpha_i}{(T_{0i}/T_{0e})\Gamma_0(\alpha_e)}, \quad (19)$$

which increases sharply with α_i due to $\Gamma_0(\alpha_e)$ for small wavelength regime ($k_\perp\rho_i > 1$), as illustrated in Figure 1.

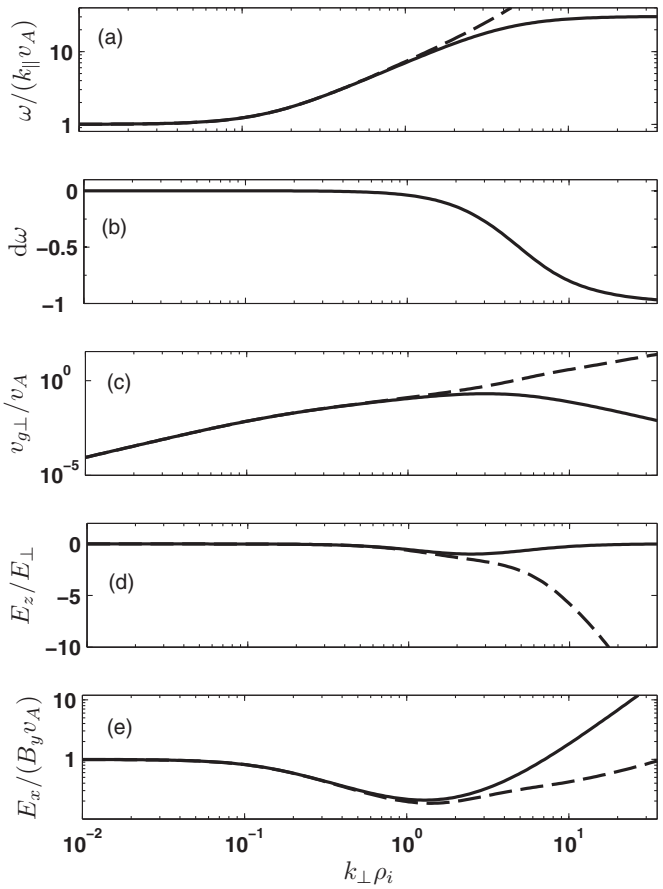

Figure 1. (a) Dependence of the normalized KAW frequency $\omega/(k_\parallel v_A)$, (b) relative difference in the wave frequency $d\omega$, (c) wave group velocity $v_{g\perp}/v_A$, (d) electric filed ratio $E_z/E_\perp$, (e) and electric/magnetic field ratio $E_x/(B_y v_A)$ on the normalized transverse wavenumber $k_\perp \rho_i$ for an ion/electron temperature ratio $T_{0i}/T_{0e} = 0.01$ and ion plasma $\beta_i = 0.01$. Plotted are analytical solutions to the two-fluid model (solid line) and gyrokinetic model (dashed line). Here, the propagation angle $\theta = 89^\circ$.

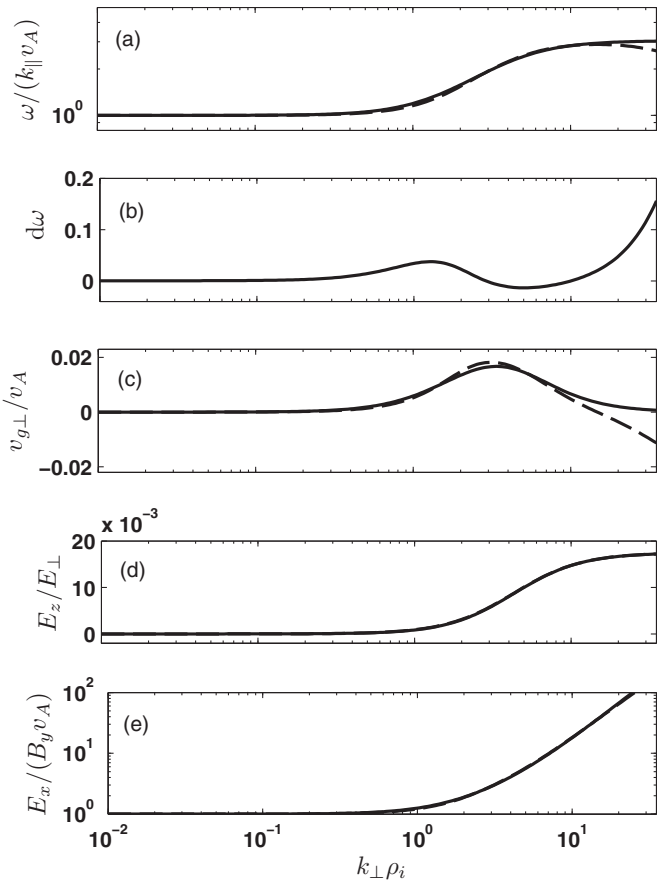

Figure 2. Same as Figure 1, but for $T_{0i}/T_{0e} = 100$.

Because other terms in Equations (18) and (19) are the same, it is $\Gamma_0(\alpha_e)$ in Equation (19), indicating the effect of electron gyroradius, that mainly causes the apparent difference between the two-fluid and gyrokinetic models. From the expression $\rho_i/\rho_e = \sqrt{(m_i/m_e)(T_{0i}/T_{0e})}$, it is clear that a low T_{0i}/T_{0e} generally corresponds to a relatively low ρ_i/ρ_e or a narrow wavelength scale interval between ρ_i and ρ_e, in which the electron gyroradius will become gradually more important. For example, in Figure 1 the condition of $T_{0i}/T_{0e} = 0.01$ gives $\rho_i/\rho_e \simeq 4.3$, both models are invalid even at $k_\perp \rho_i \simeq 4.3$, where the electron gyroscale is reached and the relative frequency difference $|d\omega| \simeq 43\%$.

For a low β_i limit (i.e., $\beta_i \sim m_e/m_i \ll 1 \ll T_{0i}/T_{0e}$, Figure 2), both models are compatible with each other better than for the finite β_i limit not only when $k_\perp \rho_i < 1$ but also when $k_\perp \rho_i \geqslant 1$. The relative frequency difference $d\omega$ is about 10% at $k_\perp \rho_i = 28.51$, and then becomes a little more obvious with shorter wavelengths. Although the sign of $d\omega$ in the short wavelength regime is positive, the wave frequencies derived from the two models are nearly the same over a wider wavelength range than those in the finite β_i limit. We also noted that, in the same β_i limit, the analytical solution to the gyrokinetic model of KAWs for $T_{0i}/T_{0e} = 100$ or $\rho_i/\rho_e = 430$ agrees well with the numerical solution to the full linear gyrokinetic one (see Figure 10 in Howes et al. 2006), which implies that the two-fluid dispersion also agrees well with the full linear gyrokinetic dispersion in this case, and that the two-fluid model of KAWs still works for wavelengths much smaller than ρ_i due to a wider scale interval (i.e., $\rho_i/\rho_e = 430$). As are the differences in the electromagnetic polarizations $E_z/E_\perp$ and $E_x/(B_y v_A)$ between the two-fluid and gyrokinetic models.

For an even lower β_i case (e.g., $\beta_i = 0.001$, same wave solutions as for the low β_i limit, Figure 3), the wave dispersion relation of the gyrokinetic model becomes more complex with an oscillation-like structure (Figure 3(a)) than those in Figures 1 and 2, making the group velocity also have a similar structure (Figure 3(b)) due to their inherent physical relation $v_{g\perp} \equiv \partial\omega/\partial k_\perp$. The appearance of the oscillation-like structure of the gyrokinetic dispersion relation is determined mainly by the low β_i effect. However, the change in the frequency difference $d\omega$ with $k_\perp \rho_i$ and the differences in $E_z/E_\perp$ and $E_x/(B_y v_A)$ between both models are similar to those in Figure 2, that is to say, the two-fluid and gyrokinetic models of KAWs agree very well within acceptable error limits ($|d\omega| \leqslant 10\%$) in this case, even for wavelengths much smaller than the ion gyroradius. For the case of $T_{0i}/T_{0e} = 10$ and $\beta_i = 0.001$, the gyrokinetic dispersion relation also has such an oscillation-like structure (listed in Table 1), and the same conclusions can be drawn here.

In the low β_i limit, the behavior of the KAWs for both models can be also explained analytically. Here the high $T_{0i}/T_{0e} \gg 1$ limit is allowed, the two-fluid dispersion relation (1) can be written as

$$\bar{\omega}^2_{2-\mathrm{fluid}} = \frac{1+\alpha_i}{1+\alpha_i \Big/ \left(\frac{\beta_i}{2}\frac{m_i}{m_e}\right)}. \quad (20)$$

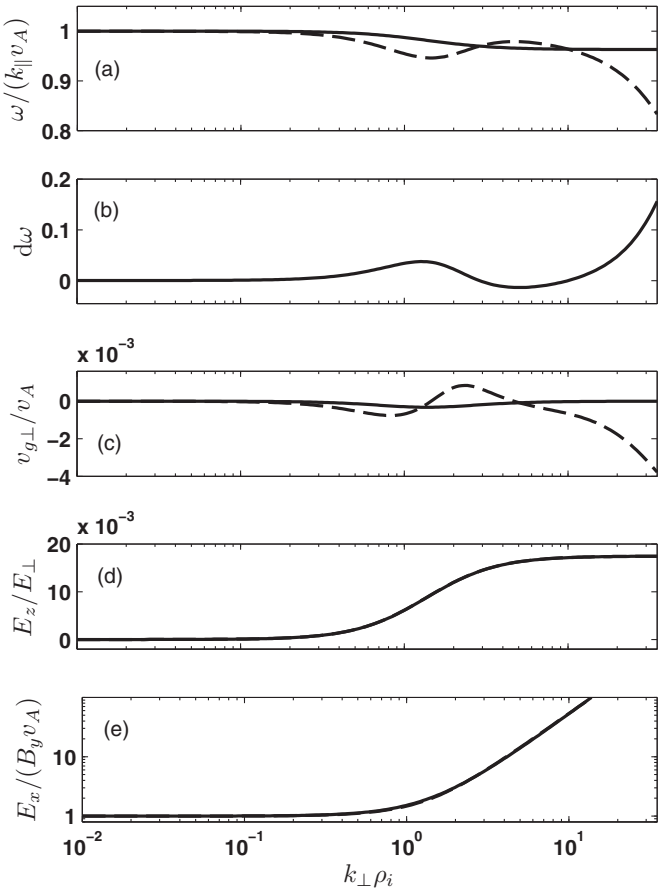

Figure 3. Same as Figure 2, but for $\beta_i = 0.001$.

Moreover, for $\alpha_i \sim O(1)$ and $\alpha_e \ll 1$ the gyrokinetic dispersion relation (15) in the same temperature limit will be

$$\bar{\omega}^2_{\rm gyrokinetic} = \frac{\alpha_i}{\left[1 + \alpha_i \Big/ \left(\frac{\beta_i}{2}\frac{m_i}{m_e}\right)\right][1 - \Gamma_0(\alpha_i)]}. \quad (21)$$

If the condition $\Gamma_0^2(\alpha_i) \ll 1$ is met, Equation (21) can be simplified as

$$\bar{\omega}^2_{\rm gyrokinetic} = \frac{[1 + \Gamma_0(\alpha_i)]\alpha_i}{1 + \alpha_i \Big/ \left(\frac{\beta_i}{2}\frac{m_i}{m_e}\right)}. \quad (22)$$

The two-fluid dispersion relation (20) and the gyrokinetic dispersion relation (22) are similar, in the same order, and quantitatively consistent with each other within acceptable error limits, as shown in Figures 2 and 3. The difference between Equations (20) and (22) is mainly due to the ring averages for protons in gyrokinetics contained in $\Gamma_0(\alpha_i)$, which is a fundamental difference between the fluid and gyrokinetic methods. Further approximation of $k_\perp\rho_i \gg 1$ and still $k_\perp\rho_e \ll 1$ (i.e., $\alpha_i \gg 1$ and $\alpha_e \ll 1$) makes both the two-fluid and gyrokinetic dispersion relations have the same form as

$$\bar{\omega}^2 = \frac{\beta_i}{2}\frac{m_i}{m_e}, \quad \text{or } \omega/k_\parallel = \sqrt{T_{0i}/m_e}, \quad (23)$$

which implies that the wave phase speed matches the electron acoustic speed in this case. Similarly, a high T_{0i}/T_{0e} usually corresponds to a relatively high ρ_i/ρ_e or a wide wavelength scale interval between ρ_i and ρ_e, in which the electron gyroradius may not be as important as the case of a low T_{0i}/T_{0e} with a narrow wavelength scale interval. For example, if $T_{0i}/T_{0e} = 100$ (adopted in Figures 2 and 3), then $\rho_i/\rho_e \simeq 430$. In this case, $k_\perp\rho_e \simeq 0.05$ even when $k_\perp\rho_i = 20$. The related $|d\omega| \simeq 5\%$ in Figures 2 and 3, showing good agreement between the fluid and gyrokinetic models for such short wavelengths. In fact, the interaction between $\Gamma_0(\alpha_i)$ and $\Gamma_0(\alpha_e)$ in the gyrokinetic dispersion relation (15) makes the detailed behavior of the KAW dispersion more complicated (see Figures 2 and 3) than what we expect from the asymptotic expression (23) of both models in the short wavelength regime $k_\perp\rho_i \gtrsim 1$, although the difference between them is small compared with the difference in the low T_{0i}/T_{0e} case.

Table 1
Cases for Comparison of Two-fluid with Gyrokinetic Models

Limit	T_{0i}/T_{0e}	β_i	ρ_i/ρ_e	$k_\perp\rho_i$[a]	Sign of $d\omega$[b]
Finite β_i limit	0.01	0.001	4.3	0.66	–
$(m_e/m_i)(T_{0i}/T_{0e}) \ll \beta_i \ll 1$	0.01	0.01	4.3	1.68	–
	0.05	0.001	9.6	0.68	–
	0.05	0.01	9.6	1.98	–
	0.1	0.001	14	0.68	–
	0.1	0.01	14	2.06	–
	0.5	0.01	30	2.15	–
	1	0.01	43	2.24	–
Low β_i limit	10	0.001	136	20.54	+[c]
$\beta_i \sim m_e/m_i \ll 1 \ll T_{0i}/T_{0e}$	10	0.01	136	20.54	+
	100	0.001	429	28.51	+[c]
	100	0.01	429	28.51	+

Notes.
[a] At which the relative difference $|d\omega| = 10\%$ and begins to increase with $k_\perp\rho_i$.
[b] When $|d\omega|$ is near or larger than 10%.
[c] With an oscillation-like structure in the gyrokinetic dispersion relation of KAWs.

More cases of the finite and low β_i limits are listed in Table 1, and have the same features as the finite and low β_i limits discussed above (Figures 1–3). It is clear that, within acceptable error limits ($|d\omega| \leqslant 10\%$), the two-fluid and gyrokinetic models agree well with shorter wavelengths (i.e., $k_\perp\rho_i \gg 1$, much shorter than the ion gyroradius but still not too close to the electron gyroscale) for a high ion/electron temperature ratio ($T_{0i}/T_{0e} \gg 1$), in which the ion gyroradius effect is dominant but the electron gyroradius effect can be ignored due to high values of $\rho_i/\rho_e > 100$ or a wide wavelength scale interval between ρ_i and ρ_e, further indicating that the two-fluid model of KAWs works well at scales much smaller than the ion gyroscale for a relatively high T_{0i}/T_{0e} and meanwhile the electromagnetic polarizations in both models are consistent well with each other. For a moderate or low ion/electron temperature ratio ($T_{0i}/T_{0e} \lesssim 1$) with $\beta_i = 0.01$, both models still agree well at ion gyroscale ($k_\perp\rho_i \sim 1$) due to the same reason. However, for the finite β_i limit (i.e., $(m_e/m_i)(T_{0i}/T_{0e}) \ll \beta_i \ll 1$) with a lower value of $\beta_i = 0.001$, both models are consistent with previous theoretical predictions that the two-fluid model holds when $k_\perp\rho_i \ll 1$ (e.g., Schekochihin et al. 2009, and references therein) and are quite different when $k_\perp\rho_i > 1$. It should also be noted that when $|d\omega| \gtrsim 10\%$, the wave frequency derived from the two-fluid model is larger ($d\omega > 0$) and smaller ($d\omega < 0$) than that from the gyrokinetic model for the low β_i limit and the finite β_i limit, respectively. The two-fluid model we used ignores the electron gyroradius effect but retains the

electron temperature and inertia and the proton gyroradius, so the deviation between the two-fluid and gyrokinetic models at subproton scales derives mainly from the electron gyroradius effect besides those caused by the usual integration of the distribution function over velocity space and ring averages of particles in gyrokinetic theory.

5. DISCUSSION

The plasma β and the ion/electron temperature ratio (T_{0i}/T_{0e}) are two important plasma parameters, and are shown to greatly affect the propagation and the polarization states of KAWs (e.g., Wu 2003; Chen & Wu 2011). We shall estimate separately the two parameters appropriate for potential applications of the two-fluid and gyrokinetic descriptions of KAWs in various solar and space plasma environments.

Firstly, low β plasmas are quite common in both the solar atmosphere and the Earth's near space environment, implying the possibility that both our two-fluid model and the gyrokinetics in the low β limit may be applied to these regions. For example, in the chromosphere β can be $<3\times10^{-2}$ close to the photosphere at $\sim$2 Mm (Gary 2001). It is also expected that magnetic flux tubes (or plasma loops) with $\beta < 10^{-3}$ may exist pervasively in the low corona, particularly near solar active regions (Wu 2005). Inside the base of a solar plume, β is about 4×10^{-3} (Deforest et al. 1997) for a density of $\sim10^{10}$ cm^{-3} (Walker et al. 1993), electron temperature of 10^6 K, and a magnetic field of 100 G. Around the top of the coronal loops above a sunspot region, the temperature is typically $\sim3\times10^6$ K, higher than that at the legs of the loops by a factor of 1.5–2.0. At the loop top, if we take $n_e = 5.3\times10^9$ cm^{-3}, $T_{0e} = 3.0\times10^6$ K, then $\beta_{\rm top} = 1.1\times10^{-3}$ for $B = 225$ G. Similarly, at loop legs, if we take $n_e = 3.5\times10^9$ cm^{-3}, $T_{0e} = 2.0\times10^6$ K, then $\beta_{\rm leg} = 1.1\times10^{-3}$ for $B = 150$ G, where the parameters of coronal loops are adopted from Fang et al. (1997) and Wu & Fang (1999). In the distant Earth's magnetotail, an ISEE 3 study (Slavin et al. 1985) of average and substorm conditions showed $\beta = 0.02$–0.05 at $|X| = 200$–$220\ R_E$ in the tail lobe. Based on these values of plasma β, it is thus likely to apply the two-fluid and gyrokinetic models of KAWs to such low-β plasma surroundings mentioned above.

Secondly, the ion/electron temperature ratio T_{0i}/T_{0e} has a wide range of values in different solar and space plasma regions. In solar coronal holes, observations suggested that some regions have proton kinetic temperature 4–10 times higher than the expected electron temperature at the same heights (Kohl et al. 1996). In some coronal mass ejections (CMEs), measurements of the Unified Radio and Plasma Wave experiment of the *Ulysses* spacecraft showed that the electron temperature is greater than the proton temperature, and sometimes they are comparable, $0.1 < T_{0i}/T_{0e} < 1$ (Lin et al. 1999), similar to the case of some interplanetary coronal mass ejection events (Hu et al. 2013). But in magnetic clouds and in the solar wind, the temperature ratio (T_{0i}/T_{0e}) is very low and ranges from 0.05 to 0.5 as shown in previous studies (e.g., Richardson et al. 1997; Sittler & Burlaga 1998; Skoug et al. 2000; Nieves-Chinchilla & Viñas 2008), and from 0.2 to 0.67 (Newbury et al. 1998), respectively. Then in the near-Earth magnetotail ($<20\ R_E$), a comprehensive statistical study of the plasma sheet using *Active Magnetospheric Particle Tracer Explorers* satellite data showed that more than 80% of the particle data measurements fell within the range $5.5 < T_{0i}/T_{0e} < 11$ (Baumjohann et al. 1989). Also, there appears to be significant deviations of the ion temperature toward values consistently less than the electron temperature in the ionosphere (Banks 1967; Bilitza 1991), but in the polar cap ionosphere and low-altitude magnetosphere data from the Intercosmos satellites and European Incoherent Scatter Svalbard radar showed that T_{0i}/T_{0e} is in the range 1–3 (Kitamura et al. 2011). It is obvious that these different values of the ion/electron temperature ratio, similar to the cases analyzed in Section 4 and listed in Table 1, indicate the validity for possible consistency of the two-fluid with gyrokinetic models of KAWs in these various solar and space plasma environments.

Furthermore, Alfvén waves have been observed as one of the most predominant low-frequency electromagnetic modes in the lower solar atmosphere (De Pontieu et al. 2007; Jess et al. 2009), and KAWs can be produced by the inhomogeneity, the parametric instability, or the nonlinear wave–wave coupling (e.g., Shukla & Sharma 2001; Shukla et al. 2004; Voitenko et al. 2003; Voitenko & Goossens 2004) when Alfvén waves propagate outward. In the surrounding coronal hole, it was shown that KAWs can be free of the strong damping and can develop into solitary nonlinear wavelets of KAWs (Wu & Yang 2007). Based on the two-fluid model, theoretical studies found that KAW heating is a more promising candidate that dominates sunspot chromospheric heating than acoustic wave heating does in the upper chromosphere above 850 km (Wu & Fang 2007), that the kinetic dissipation of KAWs has the best heating efficiency in the main body of the plume and can provide enough energy to fuel the bright coronal plume (Wu & Fang 2003), and that KAWs can produce the preferential heating and temperature anisotropy of heavy ions observed by UVCS/SOHO in the extended solar corona (Wu & Yang 2006, 2007). Although KAWs cannot be observed directly in the solar atmosphere by state-of-the-art techniques of astronomical observations, they have been found in various space plasmas by many experiments, such as in the auroral zone by sounding rocket flights (e.g., Boehm et al. 1990), *Freja* (e.g., Louarn et al. 1994; Wahlund et al. 1994), and *FAST* spacecraft (e.g., Chaston et al. 1999), in the plasma sheet boundary layer by Polar (Wygant et al. 2002), and recently in the neutral sheet by Cluster (Chaston et al. 2009). These observations of KAWs not only provide theoretical models with useful implications and additional constraints, but also prove the two-fluid description of KAWs valid in the cases mentioned above. Our results from the comparison of the two-fluid with gyrokinetic models imply that it is reasonable for us to apply both models to the KAW phenomena observed in those low-β plasma environments of the solar and space plasma systems.

Finally, what we should mention here is the respective assumptions made in the fluid and gyrokinetic models, which can cause some important differences and their corresponding pros and cons. The fluid variables are meaningful, and fluid equations are useful only when species are in thermal equilibrium states and can remain in quasi-thermal equilibrium states after they interact with the waves (i.e., Lee & Büchner 2010). The two-fluid model considers proton and electron species as separate, interacting fluids, and thus cannot describe Landau damping, particle trapping, and other kinetic effects (e.g., Lee & Büchner 2010), reflecting fundamental differences between the fluid and kinetic approaches. Schekochihin et al. (2009) mentioned that one important condition for two-fluid equations to hold is $k_\perp\rho_i \ll 1$, and that the gyrokinetic theory holds for $k_\parallel \ll k_\perp$ (anisotropy of the fluctuations) and the low frequency limit (wave frequency $\ll$ ion gyrofrequency), retaining some main kinetic effects (i.e., collisionless damping). However, our

results show that the two-fluid model (also assuming the low frequency limit) can still work well for KAWs with wavelengths comparable to or smaller than the ion gyroradius for special values of β and ion/electron temperature ratio suitable for the solar and space plasma environments, which may improve our understanding of the applicability of the two-fluid model of KAWs.

6. SUMMARY

In this paper, we compare the two-fluid and gyrokinetic descriptions of low-frequency ($\ll$ ion gyrofrequency) KAWs in the low β_i ($\ll 1$) solar and space plasma environments. From the linear KAW dispersion relation for gyrokinetics given by Howes et al. (2006), we obtain the analytical expressions of the wave group velocity and electromagnetic polarizations. The comparison results provide a confirmation of previous theoretical predictions that the two-fluid model holds when $k_\perp \rho_i \ll 1$. Even more important, the results of the two-fluid model, within acceptable error limits ($|d\omega| \leqslant 10\%$), are in reasonable agreement with those of the gyrokinetic model for KAWs with wavelengths comparable to and much shorter than the ion gyroradius ρ_i but still much larger than the electron gyroradius for a moderate or low ($\lesssim 1$) and a high ($\gg 1$) ion/electron temperature ratio, respectively. Meanwhile, the plasma β_i can make the gyrokinetic dispersion relation of KAWs become complex and sometimes have an oscillation-like structure.

Due to the inherent simplicity of the fluid theory, the comparison results may improve our understanding of the applicability of the two-fluid model, and have important implications for computer simulation studies of KAWs in various solar and space plasma phenomena. Moreover, of many astrophysical plasmas to which the results may be applied, space and solar plasmas seem to be the most suitable test beds for directly detailed quantitative comparisons of both models with observational evidence because of the high quality of a lot of measurements. The ability of the simpler two-fluid model in capturing the essential features of KAWs therein is important and bodes well for the future of the wave study and codes alike due to its very low computational cost compared with the gyrokinetic approach.

However, the fluid model depends strongly on the assumptions made to reduce a kinetic problem to a macroscopic one. A complete theoretical description of the physics governing the plasma dynamics must necessarily take into account the smallest scales and the corresponding velocity distribution functions. Sometimes low-frequency kinetic effects are shown to be important and should be included within a fluid description, even at large scales (Hunana et al. 2013). Furthermore, if the viscous and resistive effects are also considered in the fluid theory, more complicated models, such as the Landau-fluid model (Snyder et al. 1997; Passot & Sulem 2007), should be examined theoretically and numerically to adequately describe such kinetic effects and be compared to gyrokinetics or fully kinetic models in detail.

As we see, the fluid models have their limitations and uncertainties, which may be overcome by a kinetic description. Therefore, fluid model results still need to be tested systematically through using kinetic models as a reference when they are applied to new observations of solar and space plasmas. In the meantime one should always check whether the assumptions made by both models are valid and carefully select the right model for the problem to investigate, and the comparison of the model results with observational data will determine whether the models and their future progress are able to explain the observations sufficiently.

This work was supported in part by NSFC (grants 10803020, 41074107, and 11373070), the Opening Project of Key Laboratory of Solar Activity, Chinese Academy of Sciences (grant KLSA201223), and MSTC (grant 2011CB811402). S.J.W. was supported by MSTC (grant 2011CB811401) and NSFC (grant 11221063), and L.C.L. was supported by NSC of Taiwan (grant NSC 101-378 2628-M-001-007-MY3). The authors thank the referee for helpful suggestions on revising the paper.

REFERENCES

Alexashov, D., & Izmodenov, V. 2005, A&A, 439, 1171
Assis, A. S., & Busnardo-Neto, J. 1987, ApJ, 323, 399
Banks, P. M. 1967, JGR, 72, 3365
Barnes, A. 1966, PhFl, 9, 1483
Baumjohann, W., Paschmann, G., & Cattell, C. A. 1989, JGR, 94, 6597
Bellan, P. M. 2012, JGR, 117, A12219
Bernstein, I. B., & Trehan, S. K. 1960, NucFu, 1, 3
Bilitza, D. 1991, AdSpR, 11, 183
Bodo, G., & Ferrari, A. 1982, A&A, 114, 394
Boehm, M. H., Carlson, C. W., McFadden, J. P., Clemmons, J. H., & Mozer, F. S. 1990, JGR, 95, 12157
Boehm, M. H., Clemmons, J., & Paschmann, G. 1995, GeoRL, 22, 69
Brackbill, J. U. 2011, PhPl, 18, 032309
Braginskii, S. I. 1957, SPhD, 2, 345
Brizard, A. 1992, PhFlB, 4, 1213
Cao, F., & Kan, J. R. 1987, JGR, 92, 3397
Catto, P. J. 1978, PlPh, 20, 719
Chandran, B. D. G., Dennis, T. J., Quataert, E., & Bale, S. D. 2011, ApJ, 743, 197
Chandran, B. D. G., Quataert, E., Howes, G. G., Xia, Q., & Pongkitiwanichakul, P. 2009, ApJ, 707, 1668
Chaston, C. C., Carlson, C. W., Peria, W. J., Ergun, R. E., & McFadden, J. P. 1999, GeoRL, 26, 647
Chaston, C. C., Genot, V., Bonnell, J. W., et al. 2006, JGR, 111, 3206
Chaston, C. C., Johnson, J. R., Wilber, M., et al. 2009, PhRvL, 102, 015001
Chen, L., & Wu, D. J. 2011, PhPl, 18, 072110
Das, A. C., & Ip, W. H. 1992, P&SS, 40, 1499
de Assis, A. S., & de Azevedo, C. A. 1993, A&A, 271, 675
de Assis, A. S., & Leubner, C. 1994, A&A, 281, 588
de Assis, A. S., & Tsui, K. H. 1991, ApJ, 366, 324
de Azevedo, C. A., Elfimov, A. G., & de Assis, A. S. 1994, SoPh, 153, 205
De Pontieu, B., McIntosh, S. W., Carlsson, M., et al. 2007, Sci, 318, 1574
Deforest, C. E., Hoeksema, J. T., Gurman, J. B., et al. 1997, SoPh, 175, 393
Diomede, P., Michau, A., Redolfi, M., et al. 2008, PhPl, 15, 103505
Dobrowolny, M., & Torricelli-Ciamponi, G. 1985, A&A, 142, 404
Dubin, D. H. E., Krommes, J. A., Oberman, C., & Lee, W. W. 1983, PhFl, 26, 3524
Echim, M. M., Lemaire, J., & Lie-Svendsen, Ø. 2011, SGeo, 32, 1
Fang, C., Tang, Y. H., Ding, M. D., et al. 1997, SoPh, 176, 267
Farrell, W. M., Curtis, S. A., Desch, M. D., & Lepping, R. P. 1992, JGR, 97, 4133
Ferraro, N. M. 2007, ApJ, 662, 512
Formisano, V., & Kennel, C. F. 1969, J. PlPh, 3, 55
Frieman, E. A., & Chen, L. 1982, PhFl, 25, 502
Gary, G. A. 2001, SoPh, 203, 71
Goertz, C. K. 1984, P&SS, 32, 1387
Goertz, C. K. 1985, SSRv, 42, 499
Goertz, C. K., & Smith, R. A. 1989, JGR, 94, 6581
Hasegawa, A. 1976, JGR, 81, 5083
Hasegawa, A., & Chen, L. 1975, PhRvL, 35, 370
Hasegawa, A., & Mima, K. 1978, JGR, 83, 1117
Hasegawa, A., & Uberoi, C. 1982, The Alfvén Wave (Oak Ridge, TN: U.S. Department of Energy Technical Information Center)
Heyvaerts, J., & Priest, E. R. 1983, A&A, 117, 220
Hollweg, J. V. 1999, JGR, 104, 14811
Howes, G. G. 2009, NPGeo, 16, 219
Howes, G. G., Bale, S. D., Klein, K. G., et al. 2012, ApJL, 753, L19
Howes, G. G., Cowley, S. C., Dorland, W., et al. 2006, ApJ, 651, 590
Howes, G. G., Cowley, S. C., Dorland, W., et al. 2008a, JGR, 113, 5103

Howes, G. G., Dorland, W., Cowley, S. C., et al. 2008b, PhRvL, 100, 065004
Howes, G. G., & Quataert, E. 2010, ApJL, 709, L49
Howes, G. G., Tenbarge, J. M., & Dorland, W. 2011a, PhPl, 18, 102305
Howes, G. G., Tenbarge, J. M., Dorland, W., et al. 2011b, PhRvL, 107, 035004
Hu, Q., Farrugia, C. J., Osherovich, V. A., et al. 2013, SoPh, 284, 275
Hui, C. H., & Seyler, C. E. 1992, JGR, 97, 3953
Hunana, P., Goldstein, M. L., Passot, T., et al. 2013, ApJ, 766, 93
Ionson, J. A. 1978, ApJ, 226, 650
Ito, A., Hirose, A., Mahajan, S. M., & Ohsaki, S. 2004, PhPl, 11, 5643
Iukhimuk, A. K., & Kuts, S. V. 1990, KFNT, 6, 66
Jafelice, L. C., & Opher, R. 1987, Ap&SS, 137, 303
Janaki, M. S., Dasgupta, B., & Yoon, P. H. 2012, JGR, 117, A12201
Jess, D. B., Mathioudakis, M., Erdélyi, R., et al. 2009, Sci, 323, 1582
Karavaev, A. V., Gumerov, N. A., Papadopoulos, K., et al. 2011, PhPl, 18, 032113
Kitamura, N., Ogawa, Y., Nishimura, Y., et al. 2011, JGR, 116, 8227
Kletzing, C. A. 1994, JGR, 99, 11095
Kohl, J. L., Strachan, L., & Gardner, L. D. 1996, ApJL, 465, L141
Krauss-Varban, D., Omidi, N., & Quest, K. B. 1994, JGR, 99, 5987
Kucherenko, V. P., & Yukhimuk, A. K. 1993, KFNT, 9, 41
Kumar Dwivedi, N., & Sharma, R. P. 2013, PhPl, 20, 042308
Kuts, S. V., & Iukhimuk, A. K. 1990, KFNT, 6, 48
Landau, L. 1946, J. Phys. (USSR), 10, 25
Leamon, R. J., Smith, C. W., Ness, N. F., & Wong, H. K. 1999, JGR, 104, 22331
Lee, K. W., & Büchner, J. 2010, PhPl, 17, 042308
Lin, N., Kellogg, P. J., Goetz, K. A., Monson, S. J., & MacDowall, R. J. 1999, in AIP Conf. Ser. 471, ed. S. T. Suess, G. A. Gary, & S. F. Nerney (Melville, NY: AIP), 673
Louarn, P., Wahlund, J. E., Chust, T., et al. 1994, GeoRL, 21, 1847
Lysak, R. L., & Carlson, C. W. 1981, GeoRL, 8, 269
Lysak, R. L., & Lotko, W. 1996, JGR, 101, 5085
Lyu, L. H., & Kan, J. R. 1989, JGR, 94, 6523
Marchenko, V. A., Denton, R. E., & Hudson, M. K. 1996, PhPl, 3, 3861
Metzler, N., Cuperman, S., Dryer, M., & Rosenau, P. 1979, ApJ, 231, 960
Newbury, J. A., Russell, C. T., Phillips, J. L., & Gary, S. P. 1998, JGR, 103, 9553
Nielson, K. D., Howes, G. G., Tatsuno, T., Numata, R., & Dorland, W. 2010, PhPl, 17, 022105
Nieves-Chinchilla, T., & Viñas, A. F. 2008, JGR, 113, 2105
Numata, R., Dorland, W., Howes, G. G., et al. 2011, PhPl, 18, 112106
Numata, R., Howes, G. G., Tatsuno, T., Barnes, M., & Dorland, W. 2010, JCoPh, 229, 9347
Ofman, L., & Davila, J. M. 1995, JGR, 100, 23413
Parker, E. N. 2010, in Twelfth International Solar Wind Conference, ed. M. Maksimovic et al. (New York, NY: AIP Publishing), 1216, 3
Passot, T., & Sulem, P. L. 2006, JGR, 111, 4203
Passot, T., & Sulem, P. L. 2007, PhPl, 14, 082502
Podesta, J. J., Borovsky, J. E., & Gary, S. P. 2010, ApJ, 712, 685
Ren, H., Cao, J., Wu, Z., & Chu, P. K. 2011, PPCF, 53, 065021
Richardson, I. G., Farrugia, C. J., & Cane, H. V. 1997, JGR, 102, 4691
Rutherford, P. H., & Frieman, E. A. 1968, PhFl, 11, 569
Sagdeev, R. Z., & Shafranov, V. D. 1958, in Proc. Second United Nations Int. Conf. on the Peaceful Uses of Atomic Energy, Vol. 31, Geneva, 118
Sahraoui, F., Belmont, G., & Goldstein, M. L. 2012, ApJ, 748, 100
Salem, C. S., Howes, G.G., Sundkvist, D., et al. 2012, ApJL, 745, L9
Schekochihin, A. A., Cowley, S. C., Dorland, W., et al. 2009, ApJS, 182, 310
Schlüter, A. 1950, Z. Naturforsch. Teil A, 5, 72
Sharma, A. S., & Papadopoulos, K. 1995, JGR, 100, 7891
Shukla, A., & Sharma, R. P. 2001, PhPl, 8, 3759
Shukla, A., Sharma, R. P., & Malik, M. 2004, PhPl, 11, 2068
Sittler, E. C., & Burlaga, L. F. 1998, JGR, 103, 17447
Skoug, R. M., Feldman, W. C., Gosling, J. T., et al. 2000, JGR, 105, 27269
Slavin, J. A., Smith, E. J., Sibeck, D. G., Baker, D. N., & Zwickl, R. D. 1985, JGR, 90, 10875
Smith, C. W., Vasquez, B. J., & Hollweg, J. V. 2012, ApJ, 745, 8
Snyder, P. B., Hammett, G. W., & Dorland, W. 1997, PhPl, 4, 3974
Song, Y., Sazykin, S., & Wolf, R. A. 2008, JGR, 113, 8216
Spitzer, L. 1956, Physics of Fully Ionized Gases (New York: Interscience Publishers)
Stasiewicz, K., Bellan, P., Chaston, C., et al. 2000, SSRv, 92, 423
Stéfant, R. J. 1970, PhFl, 13, 440
Stringer, T. E. 1963, JNuE, 5, 89
Taylor, J. B., & Hastie, R. J. 1968, PlPh, 10, 479
TenBarge, J. M., Daughton, W., Karimabadi, H., Howes, G. G., & Dorland, W. 2014, PhPl, 21, 020708
TenBarge, J. M., Howes, G. G., & Dorland, W. 2013, ApJ, 774, 139
Thompson, B. J., & Lysak, R. L. 1996, JGR, 101, 5359
Treumann, R. A., Guedel, M., & Benz, A. O. 1990, A&A, 236, 242
Voitenko, I. M., Krishtal', A. N., Malovichko, P. P., & Iukhimuk, A. K. 1990, KFNT, 6, 61
Voitenko, Y., & Goossens, M. 2004, NPGeo, 11, 535
Voitenko, Y., Goossens, M., Sirenko, O., & Chian, A. C. L. 2003, A&A, 409, 331
Wahlund, J. E., Louarn, P., Chust, T., et al. 1994, GeoRL, 21, 1831
Walker, A. B. C., Jr., Deforest, C. E., Hoover, R. B., & Barbee, T. W., Jr. 1993, SoPh, 148, 239
Wang, D. Y., Huang, G. L., Fälthammar, C. G., et al. 1996, Ap&SS, 240, 175
Wentzel, D. G. 1979, ApJ, 233, 756
Wu, D. J. 2003, CoTPh, 39, 457
Wu, D. J. 2005, SSRv, 121, 333
Wu, D. J. 2013, Kinetic Alfvén Wave: Theory, Experiment, and Application (Beijing: Science Press)
Wu, D. J., & Chao, J. K. 2003, PhPl, 10, 3787
Wu, D. J., & Fang, C. 1999, ApJ, 511, 958
Wu, D. J., & Fang, C. 2003, ApJ, 596, 656
Wu, D. J., & Fang, C. 2007, ApJL, 659, L181
Wu, D. J., & Yang, L. 2006, A&A, 452, L7
Wu, D. J., & Yang, L. 2007, ApJ, 659, 1693
Wygant, J. R., Keiling, A., Cattell, C. A., et al. 2000, JGR, 105, 18675
Wygant, J. R., Keiling, A., Cattell, C. A., et al. 2002, JGR, 107, 1201
Yang, L., & Wu, D. J. 2005, PhPl, 12, 062903